PERGAMON

International Journal of Solids and Structures 39 (2002) 5895–5911

INTERNATIONAL JOURNAL OF SOLIDS and STRUCTURES

www.elsevier.com/locate/ijsolstr

A conducting arc crack between a circular piezoelectric inclusion and an unbounded matrix

X. Wang *, Z. Zhong

Key Laboratory of Solid Mechanics, Department of Engineering Mechanics and Technology, Tongji University, Shanghai 200092, China

Received 19 April 2002; received in revised form 25 July 2002

Abstract

The present paper investigates the problem of a conducting arc crack between a circular piezoelectric inclusion and an unbounded piezoelectric matrix. The original boundary value problem is reduced to a standard Riemann–Hilbert problem of vector form by means of analytical continuation. Explicit solutions for the stress singularities $\delta = -(1/2) \pm \mathrm{i}\varepsilon$ are obtained, closed form solutions for the field potentials are then derived through adopting a decoupling procedure. In addition, explicit expressions for the field component distributions in the whole field and along the circular interface are also obtained. Different from the interface insulating crack, stresses, strains, electric displacements and electric fields at the crack tips all exhibit oscillatory singularities. We also define a complex electro-elastic field concentration vector to characterize the singular fields near the crack tips and derive a simple expression for the energy release rate, which is always positive, in terms of the field concentration vector. The condition for the disappearance of the index ε is also discussed. When the index ε is zero, we obtain conventionally defined electro-elastic intensity factors. The examples demonstrate the physical behavior and the correctness of the obtained solution.

Keywords: Conducting arc crack; Oscillatory singularity; Energy release rate

1. Introduction

Due to their intrinsic electromechanical coupling behaviors, piezoelectric ceramics have been widely used for applications such as sensors, filters, ultrasonic generators and actuators. More recently, the use of piezoelectric materials has gone beyond the traditional application domain of small electric devices due to the emergence of piezoelectric composites. Nowadays, piezoelectric materials have been employed as integrated active structural elements. These adaptive structures are capable of monitoring and adapting to their environment, providing a "smart" response to the external conditions. Since fracture on the macro- and micro-scale can lead to undesirable mechanical and dielectric response for piezoelectric composites, fracture process of piezoelectric materials has been a subject of active research. An interface crack

* Corresponding author.
E-mail address: wjq_wang@sina.com (X. Wang).

0020-7683/02/$ - see front matter © 2002 Elsevier Science Ltd. All rights reserved.
PII: S0020-7683(02)00474-2

investigation is of paramount importance for various devices in piezoelectric composites because such cracks are often the main reason for the failure of the composite system. Kuo and Barnett (1991), Suo et al. (1992) considered the electrically conducting and electrically insulating crack faces, and singularities at the tip of an interface crack were investigated. Particularly, a singularity of a real power type was discovered around an interface crack tip for insulated crack faces. Govorukha and Loboda (2000) examined a plane strain problem for an interface crack along the fixed edge of a piezoelectric semi-infinite space. Electrically conducting and electrically insulating crack surfaces were considered in their investigation by using Fourier transforms. They found oscillatory singularities for an interface conducting crack, and introduced frictionless contact zones to eliminate the oscillatory singularities. Zhong and Meguid (1997) solved the partially debonded circular inclusion problem in piezoelectric materials with hexagonal symmetry (6 mm), which have been used for many different industrial purposes due to their high piezoelectric coupling coefficients. They derived explicit *series expressions* for the field potentials using Laurent series expansion. As pointed out by Deng and Meguid (1999), their solution was cumbersome and its convergence depends on the number of terms used in the series. More recently, Deng and Meguid (1999) reexamined the problem of a partially debonded piezoelectric circular inclusion. They obtained *closed form solutions* by considering the behavior of the complex field potentials at origin and infinity, and also derived explicit formulas for the field intensity factors. Wang and Shen (2001) considered an arc interface crack in a three-phase piezoelectric composite constitutive model. In the three-phase model, the interaction effects between neighboring inclusions can be taken into account. They obtained series form solutions for the field potentials and the field intensity factors.

In the discussions of Zhong and Meguid (1997), Deng and Meguid (1999), Wang and Shen (2001), the arc-shaped crack surfaces were assumed to be insulating or "vacuum abutted". The conducting arc crack case or the "electrode" case, in which the void inside the crack is a stress-free, conducting included phase, is also of theoretical and practical interest since dielectric break down is often associated with growth of conducting cracks. To our knowledge, this problem has not been investigated in detail. Therefore, this paper presents a systematic analysis of a conducting arc crack between a circular piezoelectric inclusion and an unbounded piezoelectric matrix. Using the analytical continuation method of Muskhelishvili (1953), the boundary value problem is reduced to a standard Riemann–Hilbert problem of vector form. Then closed form solutions for the field potentials are obtained by solving the resulting Riemann–Hilbert problem through diagonalization. In addition, explicit expressions for the physical quantity distributions in the whole field and along the circular interface are also obtained. We find that the stresses, strains, electric displacements and electric fields near the crack tips all possess the oscillatory singularities $-(1/2) \pm i\varepsilon$, in which the index ε is explicitly determined by the electro-elastic properties of the circular inclusion and the matrix. We also define a complex electro-elastic field concentration vector to characterize the singular fields near the crack tips. When $\varepsilon = 0$, the conventionally defined electro-elastic field intensity factors are also obtained explicitly. Finally, several examples are shown to understand the physical behavior of the solution.

2. Basic equations

Consider a circular piezoelectric inclusion of radius R embedded in an unbounded piezoelectric matrix as shown in Fig. 1. The two-phase piezoelectric composite is subjected to remote uniform electromechanical loadings. Both the inclusion and the matrix are assumed to be transversely isotropic with the poling direction parallel to the x_3-axis. The regions occupied by the inclusion and the matrix are denoted respectively as S_1 and S_2. The interface between S_1 and S_2 is $L = L_c \cup L_b$, where $L_c = \overset{\frown}{ab}$ represents the cracked part which is electrically conducting and traction-free, while L_b is the ideally bonded part of L. In addition, it is

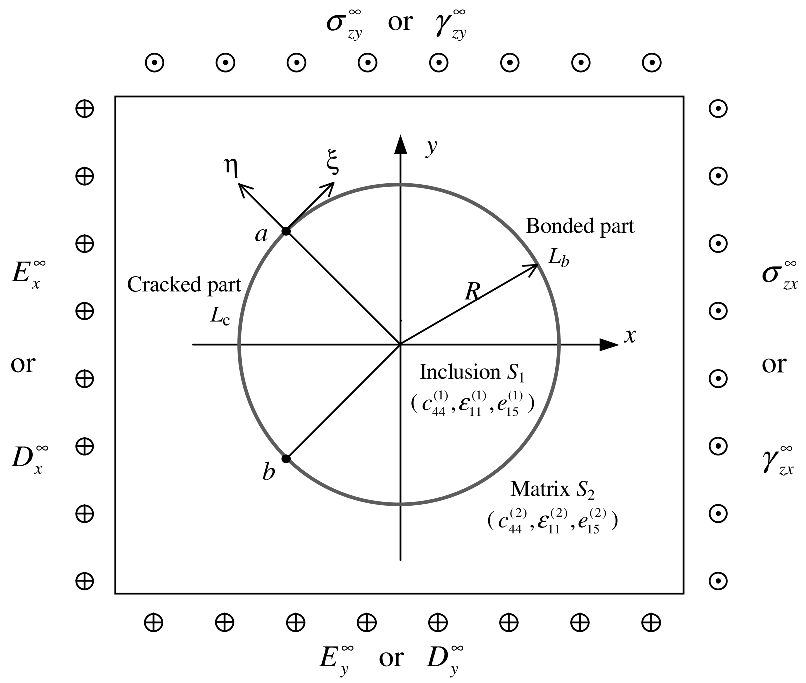

Fig. 1. A conducting arc crack between a circular piezoelectric inclusion and an infinite piezoelectric matrix.

assumed that total electric charge on L_c is zero. Without loss of generality, the centre of the arc crack lies on the *negative* x-axis and the central angle subtended by L_b is 2α. For the problem considered, the governing field equations and constitutive equations can be simplified considerably as follows

– governing field equations:

$$\sigma_{zx,x} + \sigma_{zy,y} = 0, \quad D_{x,x} + D_{y,y} = 0 \tag{1}$$

– electric field–electric potential relations:

$$E_i = -\phi_{,i} \tag{2}$$

– linear, piezoelectric constitutive equations:

$$\begin{bmatrix} \sigma_{zy} \\ D_y \end{bmatrix} = \begin{bmatrix} c_{44} & -e_{15} \\ e_{15} & \varepsilon_{11} \end{bmatrix} \begin{bmatrix} w_{,y} \\ E_y \end{bmatrix} \tag{3a}$$

$$\begin{bmatrix} \sigma_{zx} \\ D_x \end{bmatrix} = \begin{bmatrix} c_{44} & -e_{15} \\ e_{15} & \varepsilon_{11} \end{bmatrix} \begin{bmatrix} w_{,x} \\ E_x \end{bmatrix} \tag{3b}$$

where in Eqs. (1),(2),(3a),(3b), σ_{zx}, σ_{zy} are the shear stress components; D_x, D_y are the electric displacement components; E_x, E_y are the electric fields; w is out-of-plane displacement, ϕ is electric potential. c_{44}, e_{15} and ε_{11} are respectively the elastic modulus measured in a constant electric field, the piezoelectric constant, the dielectric permittivity measured at a constant strain.

For the boundary value problem discussed in this paper, it is more convenient to rewrite the above set of equations into the following equivalent ones

– governing field equations:

$$\sigma_{zx,x} + \sigma_{zy,y} = 0, \quad E_{y,x} - E_{x,y} = 0 \tag{4}$$

– linear, piezoelectric constitutive equations:

$$\begin{bmatrix} \sigma_{zy} \\ -E_x \end{bmatrix} = \begin{bmatrix} c_{44} + \frac{e_{15}^2}{\varepsilon_{11}} & 0 \\ 0 & \frac{1}{\varepsilon_{11}} \end{bmatrix} \begin{bmatrix} w_{,y} \\ \varphi_{,y} \end{bmatrix} + \begin{bmatrix} 0 & -\frac{e_{15}}{\varepsilon_{11}} \\ \frac{e_{15}}{\varepsilon_{11}} & 0 \end{bmatrix} \begin{bmatrix} w_{,x} \\ \varphi_{,x} \end{bmatrix} \tag{5a}$$

$$\begin{bmatrix} \sigma_{zx} \\ E_y \end{bmatrix} = \begin{bmatrix} c_{44} + \frac{e_{15}^2}{\varepsilon_{11}} & 0 \\ 0 & \frac{1}{\varepsilon_{11}} \end{bmatrix} \begin{bmatrix} w_{,x} \\ \varphi_{,x} \end{bmatrix} - \begin{bmatrix} 0 & -\frac{e_{15}}{\varepsilon_{11}} \\ \frac{e_{15}}{\varepsilon_{11}} & 0 \end{bmatrix} \begin{bmatrix} w_{,y} \\ \varphi_{,y} \end{bmatrix} \tag{5b}$$

where the function φ is defined in terms of the electric displacements, as follows

$$D_y = \varphi_{,x}, \quad D_x = -\varphi_{,y} \tag{6}$$

Substitution of Eqs. (5a) and (5b) into Eq. (4) results in

$$\begin{bmatrix} \nabla^2 w \\ \nabla^2 \varphi \end{bmatrix} = \mathbf{0} \quad (c_{44}\varepsilon_{11} + e_{15}^2 \neq 0) \tag{7}$$

where $\nabla^2 = \partial^2/\partial x^2 + \partial^2/\partial y^2$ is the two-dimensional Laplace operator in the variables x and y.

The general solution to the above partial differential equation (7) is

$$\mathbf{U} = \begin{bmatrix} w \\ \varphi \end{bmatrix} = \mathrm{Im}\{\mathbf{f}(z)\} \tag{8}$$

where $\mathbf{f}(z)$ is a 2-D analytic function vector of the complex variable $z = x + \mathrm{i}y$.

Then the mechanical strains and electric displacements as well as stresses and electric fields can be expressed in terms of $\mathbf{f}(z)$ as

$$\begin{bmatrix} \gamma_{zy} + \mathrm{i}\gamma_{zx} \\ -D_x + \mathrm{i}D_y \end{bmatrix} = \mathbf{f}'(z) \tag{9}$$

$$\begin{bmatrix} \sigma_{zy} + \mathrm{i}\sigma_{zx} \\ -E_x + \mathrm{i}E_y \end{bmatrix} = \mathbf{C}\mathbf{f}'(z) \tag{10}$$

in the fixed Cartesian coordinate system, and

$$\begin{bmatrix} \gamma_{z\theta} + \mathrm{i}\gamma_{zr} \\ -D_r + \mathrm{i}D_\theta \end{bmatrix} = \frac{z}{|z|}\mathbf{f}'(z) \tag{11}$$

$$\begin{bmatrix} \sigma_{z\theta} + \mathrm{i}\sigma_{zr} \\ -E_r + \mathrm{i}E_\theta \end{bmatrix} = \frac{z}{|z|}\mathbf{C}\mathbf{f}'(z) \tag{12}$$

in the polar coordinate system, where in Eqs. (10) and (12)

$$\mathbf{C} = \begin{bmatrix} c_{44} + \frac{e_{15}^2}{\varepsilon_{11}} & \mathrm{i}\frac{e_{15}}{\varepsilon_{11}} \\ -\mathrm{i}\frac{e_{15}}{\varepsilon_{11}} & \frac{1}{\varepsilon_{11}} \end{bmatrix} \tag{13}$$

Apparently, $\mathbf{C}$ is a Hermitian matrix.

Now introduce a function vector Φ, which satisfies the following relationship

$$\begin{bmatrix} \sigma_{zy} \\ -E_x \end{bmatrix} = \Phi_{,x}, \quad \begin{bmatrix} \sigma_{zx} \\ E_y \end{bmatrix} = -\Phi_{,y} \tag{14}$$

Apparently, the second component function of Φ is electric potential ϕ.

Then it follows from Eq. (10) that

$$\Phi = \mathrm{Re}\{\mathbf{C}\mathbf{f}(z)\} \tag{15}$$

Eqs. (8) and (15) can be written together into the following compact form

$$\mathbf{C}^{-1}\Phi + i\mathbf{U} = \mathbf{f}(z) \tag{16}$$

In the following analysis, the potential vector $\mathbf{f}_1(z)$ is defined in the inclusion $|z| < a$, while the potential vector $\mathbf{f}_2(z)$ is defined in the matrix $|z| > a$.

The boundary and continuity conditions on the circular interface L are

$$\begin{aligned} &\sigma_{zr}^{(1)} = \sigma_{zr}^{(2)} = 0, \quad E_\theta^{(1)} = E_\theta^{(2)} = 0, \quad \sigma \in L_\mathrm{c} \\ &\sigma_{zr}^{(1)} = \sigma_{zr}^{(2)}, \quad E_\theta^{(1)} = E_\theta^{(2)}, \quad \gamma_\theta^{(1)} = \gamma_\theta^{(2)}, \quad D_r^{(1)} = D_r^{(2)}, \quad \sigma \in L_\mathrm{b} \end{aligned} \tag{17}$$

where the superscripts “(1)” and “(2)” denote the physical quantities pertaining to the inclusion and the matrix, respectively.

The above boundary and continuity conditions on the circular interface L can be expressed in terms of the field potentials $\mathbf{f}_1(z)$ and $\mathbf{f}_2(z)$ as follows

$$\begin{aligned} &\sigma\mathbf{C}_1\mathbf{f}_1'(\sigma) - \overline{\sigma\mathbf{C}_1\mathbf{f}_1'(\sigma)} = \mathbf{0}, \quad \sigma \in L_\mathrm{c} \\ &\sigma\mathbf{C}_2\mathbf{f}_2'(\sigma) - \overline{\sigma\mathbf{C}_2\mathbf{f}_2'(\sigma)} = \mathbf{0}, \quad \sigma \in L_\mathrm{c} \\ &\sigma\mathbf{C}_1\mathbf{f}_1'(\sigma) - \overline{\sigma\mathbf{C}_1\mathbf{f}_1'(\sigma)} = \sigma\mathbf{C}_2\mathbf{f}_2'(\sigma) - \overline{\sigma\mathbf{C}_2\mathbf{f}_2'(\sigma)}, \quad \sigma \in L_\mathrm{b} \\ &\sigma\mathbf{f}_1'(\sigma) + \overline{\sigma\mathbf{f}_1'(\sigma)} = \sigma\mathbf{f}_2'(\sigma) + \overline{\sigma\mathbf{f}_2'(\sigma)}, \quad \sigma \in L_\mathrm{b} \end{aligned} \tag{18}$$

We are now in a position to determine the field potentials which satisfy the boundary and continuity conditions Eq. (18).

3. Closed form solutions for complex potentials $\mathbf{f}_1(z)$ and $\mathbf{f}_2(z)$

It follows from Eq. $(18)_{1,2,3}$ that the continuity conditions of traction and tangential component of electric fields across interface $|\sigma| = R$ can be expressed as

$$\sigma\mathbf{C}_1\mathbf{f}_1'^{+}(\sigma) - R^2/\sigma\overline{\mathbf{C}}_1\overline{\mathbf{f}}_1'^{-}(R^2/\sigma) = \sigma\mathbf{C}_2\mathbf{f}_2'^{-}(\sigma) - R^2/\sigma\overline{\mathbf{C}}_2\overline{\mathbf{f}}_2'^{+}(R^2/\sigma), \quad |\sigma| = R \tag{19}$$

Introduce a function vector $\Delta(z)$ defined by

$$\Delta(z) = \begin{cases} z\mathbf{C}_1\mathbf{f}_1'(z) + R^2/z\overline{\mathbf{C}}_2\overline{\mathbf{f}}_2'(R^2/z) - \mathbf{C}_2\mathbf{T}z - \overline{\mathbf{C}}_2\overline{\mathbf{T}}R^2/z, & |z| < a \\ R^2/z\overline{\mathbf{C}}_1\overline{\mathbf{f}}_1'(R^2/z) + z\mathbf{C}_2\mathbf{f}_2'(z) - \mathbf{C}_2\mathbf{T}z - \overline{\mathbf{C}}_2\overline{\mathbf{T}}R^2/z, & |z| > a \end{cases} \tag{20}$$

where the constant vector $\mathbf{T}$ is connected with the remote uniform electromechanical loadings, the explicit expressions for $\mathbf{T}$ can be found in the appendix.

It follows from Eqs. (19) and (20) that $\Delta(z)$ is analytic and single-valued in the whole complex plane including the points at infinity. By Liouville’s theorem, we have

$$\Delta(z) \equiv \mathbf{0} \tag{21}$$

then the following can be obtained

$$\begin{cases} R^2/z\bar{\mathbf{f}}_2'(R^2/z) = -z\overline{\mathbf{C}}_2^{-1}\mathbf{C}_1\mathbf{f}_1'(z) + \overline{\mathbf{C}}_2^{-1}\mathbf{C}_2\mathbf{T}z + \overline{\mathbf{T}}R^2/z, & |z| < a \\ R^2/z\bar{\mathbf{f}}_1'(R^2/z) = -z\overline{\mathbf{C}}_1^{-1}\mathbf{C}_2\mathbf{f}_2'(z) + \overline{\mathbf{C}}_1^{-1}\mathbf{C}_2\mathbf{T}z + \overline{\mathbf{C}}_1^{-1}\overline{\mathbf{C}}_2\overline{\mathbf{T}}R^2/z, & |z| > a \end{cases} \tag{22}$$

It follows from Eq. $(18)_4$ that the continuity condition of tangential component of mechanical strains and normal component of electric displacements across the bonded part L_b of the interface can be expressed as

$$\sigma\mathbf{f}_1'^{+}(\sigma) + R^2/\sigma\bar{\mathbf{f}}_1'^{-}(R^2/\sigma) = \sigma\mathbf{f}_2'^{-}(\sigma) + R^2/\sigma\bar{\mathbf{f}}_2'^{+}(R^2/\sigma), \quad \sigma \in L_b \tag{23}$$

Substituting Eq. (20) into Eq. (23) will yield

$$\sigma(\mathbf{I} + \overline{\mathbf{C}}_2^{-1}\mathbf{C}_1)\mathbf{f}_1'^{+}(\sigma) - \sigma(\mathbf{I} + \overline{\mathbf{C}}_1^{-1}\mathbf{C}_2)\mathbf{f}_2'^{-}(\sigma) = (\overline{\mathbf{C}}_2^{-1} - \overline{\mathbf{C}}_1^{-1})(\mathbf{C}_2\mathbf{T}\sigma + \overline{\mathbf{C}}_2\overline{\mathbf{T}}R^2/\sigma), \quad \sigma \in L_b \tag{24}$$

In view of Eq. (24), we introduce the following auxiliary function vector $\mathbf{h}(z)$

$$\mathbf{h}(z) = \begin{cases} z(\mathbf{I} + \overline{\mathbf{C}}_2^{-1}\mathbf{C}_1)\mathbf{f}_1'(z) - z(\mathbf{I} + \overline{\mathbf{C}}_2^{-1}\mathbf{C}_2)\mathbf{T}, & |z| < a \\ z(\mathbf{I} + \overline{\mathbf{C}}_1^{-1}\mathbf{C}_2)\mathbf{f}_2'(z) - z(\mathbf{I} + \overline{\mathbf{C}}_1^{-1}\mathbf{C}_2)\mathbf{T} + R^2/z(\mathbf{I} - \overline{\mathbf{C}}_1^{-1}\overline{\mathbf{C}}_2)\overline{\mathbf{T}}, & |z| > a \end{cases} \tag{25}$$

It is apparent that $\mathbf{h}(z)$ is sectionally holomorphic within the circle $|z| < a$ and outside the circle $|z| > a$, and is continuous across the bonded part L_b, i.e.,

$$\mathbf{h}^{+}(\sigma) - \mathbf{h}^{-}(\sigma) = \mathbf{0}, \quad \sigma \in L_b \tag{26}$$

in addition

$$\mathbf{h}(0) = \mathbf{0} \tag{27}$$

The traction free and equi-potential requirement $(18)_1$ or $(18)_2$ on the debonded part (crack) L_c of the interface can be expressed as

$$\sigma\mathbf{C}_1\mathbf{f}_1'^{+}(\sigma) - R^2/\sigma\overline{\mathbf{C}}_1\bar{\mathbf{f}}_1'^{-}(R^2/\sigma) = \mathbf{0}, \quad \sigma \in L_c \tag{28}$$

Using Eqs. (22) and (25), the above boundary condition can be expressed in terms of the newly defined function vector $\mathbf{h}(z)$ as follows

$$\mathbf{M}\mathbf{h}^{+}(\sigma) + \overline{\mathbf{M}}\mathbf{h}^{-}(\sigma) = \mathbf{g}(\sigma), \quad \sigma \in L_c \tag{29}$$

with

$$\mathbf{g}(\sigma) = -\sigma\mathbf{M}(\mathbf{I} + \overline{\mathbf{C}}_2^{-1}\mathbf{C}_2)\mathbf{T} + R^2/\sigma\overline{\mathbf{M}}(\mathbf{I} + \mathbf{C}_2^{-1}\overline{\mathbf{C}}_2)\overline{\mathbf{T}} \tag{30}$$

and the Hermitian matrix $\mathbf{M}$ is given by

$$\mathbf{M} = \left[\mathbf{C}_1^{-1} + \overline{\mathbf{C}}_2^{-1}\right]^{-1} \tag{31a}$$

or more specifically

$$\mathbf{M} = \frac{1}{\left(c_{44}^{(1)} + c_{44}^{(2)}\right)\left(\varepsilon_{11}^{(1)} + \varepsilon_{11}^{(2)}\right) + \left(e_{15}^{(1)} + e_{15}^{(2)}\right)^2} \times \begin{bmatrix} c_{44}^{(1)}c_{44}^{(2)}\left(\varepsilon_{11}^{(1)} + \varepsilon_{11}^{(2)}\right) + c_{44}^{(2)}e_{15}^{(1)^2} + c_{44}^{(1)}e_{15}^{(2)^2} & -i\left(c_{44}^{(1)}e_{15}^{(2)} - c_{44}^{(2)}e_{15}^{(1)}\right) \\ i\left(c_{44}^{(1)}e_{15}^{(2)} - c_{44}^{(2)}e_{15}^{(1)}\right) & c_{44}^{(1)} + c_{44}^{(2)} \end{bmatrix} \tag{31b}$$

Apparently, Eqs. (26) and (29) comprise a standard Riemann–Hilbert problem of vector form. In view of Eq. (29), we consider the following eigenvalue problem

$$(\overline{\mathbf{M}} - e^{-2\pi\varepsilon}\mathbf{M})\mathbf{v} = \mathbf{0} \tag{32}$$

Following Ting (1986), the oscillatory index ε in the above equation can be explicitly determined to be

$$\varepsilon = \pm\frac{1}{2\pi}\ln\frac{1+\beta}{1-\beta} \tag{33}$$

$$\beta = \frac{c_{44}^{(1)}e_{15}^{(2)} - c_{44}^{(2)}e_{15}^{(1)}}{\sqrt{\left(c_{44}^{(1)} + c_{44}^{(2)}\right)\left[c_{44}^{(1)}c_{44}^{(2)}\left(\varepsilon_{11}^{(1)} + \varepsilon_{11}^{(2)}\right) + c_{44}^{(2)}e_{15}^{(1)^2} + c_{44}^{(1)}e_{15}^{(2)^2}\right]}}, \tag{34}$$

while the explicit solution for eigenvector $\mathbf{v}$ associated with ε is

$$\mathbf{v} = \begin{bmatrix} \eta \\ \pm i \end{bmatrix} \tag{35}$$

with the real constant η given by

$$\eta = \sqrt{\frac{c_{44}^{(1)} + c_{44}^{(2)}}{c_{44}^{(1)}c_{44}^{(2)}\left(\varepsilon_{11}^{(1)} + \varepsilon_{11}^{(2)}\right) + c_{44}^{(2)}e_{15}^{(1)^2} + c_{44}^{(1)}e_{15}^{(2)^2}}} \tag{36}$$

From Eq. (34), we can deduce that a necessary and sufficient condition for the absence of index ε is the following

$$\frac{c_{44}^{(1)}}{c_{44}^{(2)}} = \frac{e_{15}^{(1)}}{e_{15}^{(2)}} \tag{37}$$

We find that the above condition is only dependent on elastic and piezoelectric constants of the two phases, and is independent of the dielectric constants of the two phases. The above condition is equivalent to $\mathrm{Im}\{\mathbf{M}\} = \mathbf{0}$, which is identical to that shown by Ting (1986) for purely anisotropic elastic bimaterials.

Now introduce the following coordinate transformation

$$\mathbf{h}(z) = \mathbf{P}\hat{\mathbf{h}}(z), \quad \hat{\mathbf{g}}(\sigma) = \Lambda_1\overline{\mathbf{P}}^{\mathrm{T}}\mathbf{g}(\sigma) \tag{38}$$

where

$$\mathbf{P} = \begin{bmatrix} \eta & \eta \\ i & -i \end{bmatrix} \tag{39}$$

$$\Lambda_1 = \frac{\left(c_{44}^{(1)} + c_{44}^{(2)}\right)\left(\varepsilon_{11}^{(1)} + \varepsilon_{11}^{(2)}\right) + \left(e_{15}^{(1)} + e_{15}^{(2)}\right)^2}{2\left(c_{44}^{(1)} + c_{44}^{(2)}\right)} \begin{bmatrix} \dfrac{1}{1+\beta} & 0 \\ 0 & \dfrac{1}{1-\beta} \end{bmatrix} \tag{40}$$

Premultiply Eq. (29) by $\overline{\mathbf{P}}^{\mathrm{T}}$ and utilize Eq. (38), then we can finally obtain the following decoupled Riemann–Hilbert problem

$$\hat{\mathbf{h}}^{+}(\sigma) + \Lambda\hat{\mathbf{h}}^{-}(\sigma) = \hat{\mathbf{g}}(\sigma), \quad \sigma \in L_{\mathrm{c}} \tag{41}$$

where

$$\Lambda = \begin{bmatrix} e^{-2\pi\varepsilon} & 0 \\ 0 & e^{2\pi\varepsilon} \end{bmatrix} \tag{42}$$

A general solution to Eq. (41) is (Muskhelishvili, 1953)

$$\hat{\mathbf{h}}(z) = \frac{X(z)}{2\pi i} \int_{L_c} \frac{[X^+(\sigma)]^{-1}\hat{\mathbf{g}}(\sigma)}{\sigma - z}\, d\sigma + X(z)\mathbf{c} \tag{43}$$

where the unknown constant vector $\mathbf{c}$ can be uniquely determined by Eq. (27), and

$$X(z) = \begin{bmatrix} (z-a)^{-\frac{1}{2}-i\varepsilon}(z-b)^{-\frac{1}{2}+i\varepsilon} & 0 \\ 0 & (z-a)^{-\frac{1}{2}+i\varepsilon}(z-b)^{-\frac{1}{2}-i\varepsilon} \end{bmatrix} \tag{44}$$

The above basic Plemelj function $X(z)$ has a cut along the crack L_c, in addition $X(z) = \mathbf{o}(z^{-1})$ when $z \to \infty$.

The Cauchy type integral in Eq. (43) can be exactly performed, and the final result is

$$\hat{\mathbf{h}}(z) = -(\mathbf{I}+\Lambda)^{-1}[z\mathbf{I} - z\mathbf{S}_\infty(z)]\Lambda_1\overline{\mathbf{P}}^{\mathrm{T}}\mathbf{M}(\mathbf{I}+\overline{\mathbf{C}}_2^{-1}\mathbf{C}_2)\mathbf{T} + (\mathbf{I}+\Lambda)^{-1}\left[R^2/z\mathbf{I} - z\mathbf{S}_0(z)\right]\Lambda_1\overline{\mathbf{P}}^{\mathrm{T}}\overline{\mathbf{M}}(\mathbf{I}+\mathbf{C}_2^{-1}\overline{\mathbf{C}}_2)\overline{\mathbf{T}} \tag{45}$$

where

$$\mathbf{S}_\infty(z) = X(z)\begin{bmatrix} s_{1\infty}(z) & 0 \\ 0 & s_{2\infty}(z) \end{bmatrix}, \quad \mathbf{S}_0(z) = \mathrm{X}(z)\begin{bmatrix} s_{10}(z) & 0 \\ 0 & s_{20}(z) \end{bmatrix} \tag{46}$$

with

$$\begin{aligned} s_{1\infty}(z) &= [z - R(\cos\alpha - 2\varepsilon\sin\alpha)] \\ s_{2\infty}(z) &= [z - R(\cos\alpha + 2\varepsilon\sin\alpha)] \\ s_{10}(z) &= R^2 e^{2\varepsilon(\pi-\alpha)}\left[Rz^{-2} - (\cos\alpha + 2\varepsilon\sin\alpha)z^{-1}\right] \\ s_{20}(z) &= R^2 e^{-2\varepsilon(\pi-\alpha)}\left[Rz^{-2} - (\cos\alpha - 2\varepsilon\sin\alpha)z^{-1}\right] \end{aligned} \tag{47}$$

It follows from Eq. (38) that

$$\mathbf{h}(z) = -\mathrm{P}(\mathbf{I}+\Lambda)^{-1}[z\mathbf{I} - z\mathbf{S}_\infty(z)]\Lambda_1\overline{\mathbf{P}}^{\mathrm{T}}\mathbf{M}(\mathbf{I}+\overline{\mathbf{C}}_2^{-1}\mathbf{C}_2)\mathbf{T} + \mathrm{P}(\mathbf{I}+\Lambda)^{-1}\left[R^2/z\mathbf{I} - z\mathbf{S}_0(z)\right]\Lambda_1\overline{\mathbf{P}}^{\mathrm{T}}\overline{\mathbf{M}}(\mathbf{I}+\mathbf{C}_2^{-1}\overline{\mathbf{C}}_2)\overline{\mathbf{T}} \tag{48}$$

Noting Eq. (25), then the potential vectors $\mathbf{f}_1'(z)$, $\mathbf{f}_2'(z)$ are

$$\begin{aligned} \mathbf{f}_1'(z) = &-\mathbf{C}_1^{-1}\mathbf{M}\mathrm{P}(\mathbf{I}+\Lambda)^{-1}[\mathbf{I} - \mathbf{S}_\infty(z)]\Lambda_1\overline{\mathbf{P}}^{\mathrm{T}}\mathbf{M}(\mathbf{I}+\overline{\mathbf{C}}_2^{-1}\mathbf{C}_2)\mathbf{T} \\ &+ \mathbf{C}_1^{-1}\mathbf{M}\mathrm{P}(\mathbf{I}+\Lambda)^{-1}\left[R^2/z^2\mathbf{I} - \mathbf{S}_0(z)\right]\Lambda_1\overline{\mathbf{P}}^{\mathrm{T}}\overline{\mathbf{M}}(\mathbf{I}+\mathbf{C}_2^{-1}\overline{\mathbf{C}}_2)\overline{\mathbf{T}} + \mathbf{C}_1^{-1}\mathbf{M}(\mathbf{I}+\overline{\mathbf{C}}_2^{-1}\mathbf{C}_2)\mathbf{T} \quad |z| < a \end{aligned} \tag{49}$$

$$\begin{aligned} \mathbf{f}_2'(z) = &-\mathbf{C}_2^{-1}\overline{\mathbf{M}}\mathrm{P}(\mathbf{I}+\Lambda)^{-1}[\mathbf{I} - \mathbf{S}_\infty(z)]\Lambda_1\overline{\mathbf{P}}^{\mathrm{T}}\mathbf{M}(\mathbf{I}+\overline{\mathbf{C}}_2^{-1}\mathbf{C}_2)\mathbf{T} - R^2/z^2\mathbf{C}_2^{-1}\overline{\mathbf{M}}(\mathbf{I}-\overline{\mathbf{C}}_1^{-1}\overline{\mathbf{C}}_2)\overline{\mathbf{T}} \\ &+ \mathbf{C}_2^{-1}\overline{\mathbf{M}}\mathrm{P}(\mathbf{I}+\Lambda)^{-1}\left[R^2/z^2\mathbf{I} - \mathbf{S}_0(z)\right]\Lambda_1\overline{\mathbf{P}}^{\mathrm{T}}\overline{\mathbf{M}}(\mathbf{I}+\mathbf{C}_2^{-1}\overline{\mathbf{C}}_2)\overline{\mathbf{T}} + \mathbf{T} \quad |z| > a \end{aligned} \tag{50}$$

Integrating the above two expressions will result in

$$\mathbf{f}_1(z) = -\mathbf{C}_1^{-1}\mathbf{MP}(\mathbf{I}+\Lambda)^{-1}[z\mathbf{I}-\mathbf{R}_\infty(z)]\Lambda_1\overline{\mathbf{P}}^{\mathrm{T}}\mathbf{M}(\mathbf{I}+\overline{\mathbf{C}}_2^{-1}\mathbf{C}_2)\mathbf{T} - \mathbf{C}_1^{-1}\mathbf{MP}(\mathbf{I}+\Lambda)^{-1}\left[R^2/z\mathbf{I}-\mathbf{R}_0(z)\right]\Lambda_1\overline{\mathbf{P}}^{\mathrm{T}}\overline{\mathbf{M}}(\mathbf{I}+\mathbf{C}_2^{-1}\overline{\mathbf{C}}_2)\overline{\mathbf{T}} + z\mathbf{C}_1^{-1}\mathbf{M}(\mathbf{I}+\overline{\mathbf{C}}_2^{-1}\mathbf{C}_2)\mathbf{T} \quad |z|<a \tag{51}$$

$$\mathbf{f}_2(z) = -\mathbf{C}_2^{-1}\overline{\mathbf{M}}\mathbf{P}(\mathbf{I}+\Lambda)^{-1}[z\mathbf{I}-\mathbf{R}_\infty(z)]\Lambda_1\overline{\mathbf{P}}^{\mathrm{T}}\mathbf{M}(\mathbf{I}+\overline{\mathbf{C}}_2^{-1}\mathbf{C}_2)\mathbf{T} + R^2/z\mathbf{C}_2^{-1}\overline{\mathbf{M}}(\mathbf{I}-\overline{\mathbf{C}}_1^{-1}\overline{\mathbf{C}}_2)\overline{\mathbf{T}} - \mathbf{C}_2^{-1}\overline{\mathbf{M}}\mathbf{P}(\mathbf{I}+\Lambda)^{-1}\left[R^2/z\mathbf{I}-\mathbf{R}_0(z)\right]\Lambda_1\overline{\mathbf{P}}^{\mathrm{T}}\overline{\mathbf{M}}(\mathbf{I}+\mathbf{C}_2^{-1}\overline{\mathbf{C}}_2)\overline{\mathbf{T}} + z\mathbf{T} \quad |z|>a \tag{52}$$

where

$$\begin{aligned}\mathbf{R}_\infty(z) &= \int \mathbf{S}_\infty(z)\,\mathrm{d}z = (z-a)(z-b)X(z)\\ \mathbf{R}_0(z) &= -\int \mathbf{S}_0(z)\,\mathrm{d}z = Rz^{-1}(z-a)(z-b)X(z)\begin{bmatrix} \mathrm{e}^{2\varepsilon(\pi-\alpha)} & 0 \\ 0 & \mathrm{e}^{-2\varepsilon(\pi-\alpha)}\end{bmatrix}\end{aligned} \tag{53}$$

We can also observe that the analysis of a conducting arc crack is more complicated than the analysis of an insulating arc crack (Zhong and Meguid, 1997; Deng and Meguid, 1999; Wang and Shen, 2001), with most of the difficulty stemming from resolving the coupled Riemann–Hilbert problem of vector form.

4. Explicit expressions for physical quantities

4.1. Full field distribution of physical quantities

It follows from Eqs. (9), (10) and (49), (50) that

$$\begin{bmatrix}\gamma_{zy}+\mathrm{i}\gamma_{zx}\\ -D_x+\mathrm{i}D_y\end{bmatrix} = -\mathbf{C}_1^{-1}\mathbf{MP}(\mathbf{I}+\Lambda)^{-1}[\mathbf{I}-\mathbf{S}_\infty(z)]\Lambda_1\overline{\mathbf{P}}^{\mathrm{T}}\mathbf{M}(\mathbf{I}+\overline{\mathbf{C}}_2^{-1}\mathbf{C}_2)\mathbf{T} + \mathbf{C}_1^{-1}\mathbf{MP}(\mathbf{I}+\Lambda)^{-1}\left[R^2/z^2\mathbf{I}-\mathbf{S}_0(z)\right]\Lambda_1\overline{\mathbf{P}}^{\mathrm{T}}\overline{\mathbf{M}}(\mathbf{I}+\mathbf{C}_2^{-1}\overline{\mathbf{C}}_2)\overline{\mathbf{T}} + \mathbf{C}_1^{-1}\mathbf{M}(\mathbf{I}+\overline{\mathbf{C}}_2^{-1}\mathbf{C}_2)\mathbf{T} \tag{54}$$

$$\begin{bmatrix}\sigma_{zy}+\mathrm{i}\sigma_{zx}\\ -E_x+\mathrm{i}E_y\end{bmatrix} = -\mathbf{MP}(\mathbf{I}+\Lambda)^{-1}[\mathbf{I}-\mathbf{S}_\infty(z)]\Lambda_1\overline{\mathbf{P}}^{\mathrm{T}}\mathbf{M}(\mathbf{I}+\overline{\mathbf{C}}_2^{-1}\mathbf{C}_2)\mathbf{T} + \mathbf{MP}(\mathbf{I}+\Lambda)^{-1}\left[R^2/z^2\mathbf{I}-\mathbf{S}_0(z)\right]\Lambda_1\overline{\mathbf{P}}^{\mathrm{T}}\overline{\mathbf{M}}(\mathbf{I}+\mathbf{C}_2^{-1}\overline{\mathbf{C}}_2)\overline{\mathbf{T}} + \mathbf{M}(\mathbf{I}+\overline{\mathbf{C}}_2^{-1}\mathbf{C}_2)\mathbf{T} \tag{55}$$

within the circular piezoelectric inclusion $|z| < a$, and

$$\begin{bmatrix}\gamma_{zy}+\mathrm{i}\gamma_{zx}\\ -D_x+\mathrm{i}D_y\end{bmatrix} = -\mathbf{C}_2^{-1}\overline{\mathbf{M}}\mathbf{P}(\mathbf{I}+\Lambda)^{-1}[\mathbf{I}-\mathbf{S}_\infty(z)]\Lambda_1\overline{\mathbf{P}}^{\mathrm{T}}\mathbf{M}(\mathbf{I}+\overline{\mathbf{C}}_2^{-1}\mathbf{C}_2)\mathbf{T} + \mathbf{C}_2^{-1}\overline{\mathbf{M}}\mathbf{P}(\mathbf{I}+\Lambda)^{-1}\left[R^2/z^2\mathbf{I}-\mathbf{S}_0(z)\right]\Lambda_1\overline{\mathbf{P}}^{\mathrm{T}}\overline{\mathbf{M}}(\mathbf{I}+\mathbf{C}_2^{-1}\overline{\mathbf{C}}_2)\overline{\mathbf{T}} - R^2/z^2\mathbf{C}_2^{-1}\overline{\mathbf{M}}(\mathbf{I}-\overline{\mathbf{C}}_1^{-1}\overline{\mathbf{C}}_2)\overline{\mathbf{T}} + \mathbf{T} \tag{56}$$

$$\begin{bmatrix}\sigma_{zy}+\mathrm{i}\sigma_{zx}\\ -E_x+\mathrm{i}E_y\end{bmatrix} = -\overline{\mathbf{M}}\mathbf{P}(\mathbf{I}+\Lambda)^{-1}[\mathbf{I}-\mathbf{S}_\infty(z)]\Lambda_1\overline{\mathbf{P}}^{\mathrm{T}}\mathbf{M}(\mathbf{I}+\overline{\mathbf{C}}_2^{-1}\mathbf{C}_2)\mathbf{T} + \overline{\mathbf{M}}\mathbf{P}(\mathbf{I}+\Lambda)^{-1}\left[R^2/z^2\mathbf{I}-\mathbf{S}_0(z)\right]\Lambda_1\overline{\mathbf{P}}^{\mathrm{T}}\overline{\mathbf{M}}(\mathbf{I}+\mathbf{C}_2^{-1}\overline{\mathbf{C}}_2)\overline{\mathbf{T}} - R^2/z^2\overline{\mathbf{M}}(\mathbf{I}-\overline{\mathbf{C}}_1^{-1}\overline{\mathbf{C}}_2)\overline{\mathbf{T}} + \mathbf{C}_2\mathbf{T} \tag{57}$$

within the unbounded piezoelectric matrix $|z| > a$.

4.2. Distribution of physical quantities along the interface L

It follows from Eqs. (11) and (12) and (49) and (50) that

$$\begin{bmatrix} \gamma_{z\theta}+\mathrm{i}\gamma_{zr} \\ -D_r+\mathrm{i}D_\theta \end{bmatrix}^+ = -\mathbf{C}_1^{-1}\mathbf{M}\mathbf{P}(\mathbf{I}+\Lambda)^{-1}\frac{\sigma}{R}\left[\mathbf{I}-\mathbf{S}_\infty^+(\sigma)\right]\Lambda_1\overline{\mathbf{P}}^{\mathrm{T}}\mathbf{M}(\mathbf{I}+\overline{\mathbf{C}}_2^{-1}\mathbf{C}_2)\mathbf{T} + \mathbf{C}_1^{-1}\mathbf{M}\mathbf{P}(\mathbf{I}+\Lambda)^{-1}\frac{\sigma}{R}\left[R^2/\sigma^2\mathbf{I}-\mathbf{S}_0^+(\sigma)\right]\Lambda_1\overline{\mathbf{P}}^{\mathrm{T}}\overline{\mathbf{M}}(\mathbf{I}+\mathbf{C}_2^{-1}\overline{\mathbf{C}}_2)\overline{\mathbf{T}}+\frac{\sigma}{R}\mathbf{C}_1^{-1}\mathbf{M}(\mathbf{I}+\overline{\mathbf{C}}_2^{-1}\mathbf{C}_2)\mathbf{T} \tag{58}$$

$$\begin{bmatrix} \sigma_{z\theta}+\mathrm{i}\sigma_{zr} \\ -E_r+\mathrm{i}E_\theta \end{bmatrix}^+ = -\mathbf{M}\mathbf{P}(\mathbf{I}+\Lambda)^{-1}\frac{\sigma}{R}\left[\mathbf{I}-\mathbf{S}_\infty^+(\sigma)\right]\Lambda_1\overline{\mathbf{P}}^{\mathrm{T}}\mathbf{M}(\mathbf{I}+\overline{\mathbf{C}}_2^{-1}\mathbf{C}_2)\mathbf{T} + \mathbf{M}\mathbf{P}(\mathbf{I}+\Lambda)^{-1}\frac{\sigma}{R}\left[R^2/\sigma^2\mathbf{I}-\mathbf{S}_0^+(\sigma)\right]\Lambda_1\bar{\mathbf{P}}^{\mathrm{T}}\overline{\mathbf{M}}(\mathbf{I}+\mathbf{C}_2^{-1}\overline{\mathbf{C}}_2)\overline{\mathbf{T}}+\frac{\sigma}{R}\mathbf{M}(\mathbf{I}+\overline{\mathbf{C}}_2^{-1}\mathbf{C}_2)\mathbf{T} \tag{59}$$

along the inclusion side of the interface $|\sigma| = R$, and

$$\begin{bmatrix} \gamma_{z\theta}+\mathrm{i}\gamma_{zr} \\ -D_r+\mathrm{i}D_\theta \end{bmatrix}^- = -\mathbf{C}_2^{-1}\overline{\mathbf{M}}\mathbf{P}(\mathbf{I}+\Lambda)^{-1}\frac{\sigma}{R}\left[\mathbf{I}-\mathbf{S}_\infty^-(\sigma)\right]\Lambda_1\overline{\mathbf{P}}^{\mathrm{T}}\mathbf{M}(\mathbf{I}+\overline{\mathbf{C}}_2^{-1}\mathbf{C}_2)\mathbf{T}+\mathbf{C}_2^{-1}\overline{\mathbf{M}}\mathbf{P}(\mathbf{I}+\Lambda)^{-1} \times\frac{\sigma}{R}\left[R^2/\sigma^2\mathbf{I}-\mathbf{S}_0^-(\sigma)\right]\Lambda_1\overline{\mathbf{P}}^{\mathrm{T}}\overline{\mathbf{M}}(\mathbf{I}+\mathbf{C}_2^{-1}\overline{\mathbf{C}}_2)\overline{\mathbf{T}}-\frac{R}{\sigma}\mathbf{C}_2^{-1}\overline{\mathbf{M}}(\mathbf{I}-\overline{\mathbf{C}}_1^{-1}\overline{\mathbf{C}}_2)\overline{\mathbf{T}}+\frac{\sigma}{R}\mathbf{T} \tag{60}$$

$$\begin{bmatrix} \sigma_{z\theta}+\mathrm{i}\sigma_{zr} \\ -E_r+\mathrm{i}E_\theta \end{bmatrix}^- = -\overline{\mathbf{M}}\mathbf{P}(\mathbf{I}+\Lambda)^{-1}\frac{\sigma}{R}\left[\mathbf{I}-\mathbf{S}_\infty^-(\sigma)\right]\Lambda_1\overline{\mathbf{P}}^{\mathrm{T}}\mathbf{M}(\mathbf{I}+\overline{\mathbf{C}}_2^{-1}\mathbf{C}_2)\mathbf{T}+\overline{\mathbf{M}}\mathbf{P}(\mathbf{I}+\Lambda)^{-1} \times\frac{\sigma}{R}\left[R^2/\sigma^2\mathbf{I}-\mathbf{S}_0^-(\sigma)\right]\Lambda_1\overline{\mathbf{P}}^{\mathrm{T}}\overline{\mathbf{M}}(\mathbf{I}+\mathbf{C}_2^{-1}\overline{\mathbf{C}}_2)\overline{\mathbf{T}}-\frac{R}{\sigma}\overline{\mathbf{M}}(\mathbf{I}-\overline{\mathbf{C}}_1^{-1}\overline{\mathbf{C}}_2)\overline{\mathbf{T}}+\frac{\sigma}{R}\mathbf{C}_2\mathbf{T} \tag{61}$$

along the matrix side of the interface $|\sigma| = R$.

It follows from Eqs. (8), (51) and (52) that discontinuity in w and φ on the crack L_c can be expressed as

$$\Delta\mathbf{U} = \mathbf{U}_1 - \mathbf{U}_2 = \mathrm{Im}\left\{P(\sigma-a)(\sigma-b)X^+(\sigma)\Lambda^{-1}\Lambda_1\overline{\mathbf{P}}^{\mathrm{T}}\mathbf{M}(\mathbf{I}+\overline{\mathbf{C}}_2^{-1}\mathbf{C}_2)\mathbf{T}\right\}, \quad \sigma\in L_c \tag{62}$$

Differentiating the above expression along the tangential direction of the interface will result in the following densities of dislocations $\hat{b}$ and electric charges $\hat{q}$ continuously distributed along the arc crack L_c

$$\begin{bmatrix} \hat{b} \\ \hat{q} \end{bmatrix} = \mathrm{Re}\left\{\frac{\sigma}{R}\mathbf{P}\mathbf{S}_\infty^+(\sigma)\Lambda^{-1}\Lambda_1\bar{\mathbf{P}}^{\mathrm{T}}\mathbf{M}(\mathbf{I}+\overline{\mathbf{C}}_2^{-1}\mathbf{C}_2)\mathbf{T}\right\}, \quad \sigma\in L_c \tag{63}$$

4.3. Field components near the crack tip

It can be observed from Eqs. (58)–(62) that stresses, strains, electric displacements and electric fields all possess the oscillatory singularities $-(1/2)\pm i\varepsilon$, a result different from that derived by Zhong and Meguid (1997), Deng and Meguid (1999), Wang and Shen (2001) for an insulating arc crack. Furthermore, stresses, strains, electric fields and electric displacements are singularly distributed just ahead of the upper crack tip $a = R\exp\{\mathrm{i}\alpha\}$ along the interface as follows

$$\begin{bmatrix} \gamma_{z\theta}+\mathrm{i}\gamma_{zr} \\ -D_r+\mathrm{i}D_\theta \end{bmatrix}^+ = \frac{\mathrm{i}}{\sqrt{2\pi r}}\mathbf{C}_1^{-1}\mathbf{M}\mathbf{P}\mathbf{Y}(r)\mathbf{K} \quad (r = |\sigma-a|) \tag{64}$$

$$\begin{bmatrix} \sigma_{z\theta} + \mathrm{i}\sigma_{zr} \\ -E_r + \mathrm{i}E_\theta \end{bmatrix}^+ = \frac{\mathrm{i}}{\sqrt{2\pi r}}\mathbf{MP}\mathrm{Y}(r)\mathbf{K} \quad (r = |\sigma - a|) \tag{65}$$

in the inclusion side, and

$$\begin{bmatrix} \gamma_{z\theta} + \mathrm{i}\gamma_{zr} \\ -D_r + \mathrm{i}D_\theta \end{bmatrix}^- = \frac{\mathrm{i}}{\sqrt{2\pi r}}\mathbf{C}_2^{-1}\mathbf{MP}\mathrm{Y}(r)\mathbf{K} \quad (r = |\sigma - a|) \tag{66}$$

$$\begin{bmatrix} \sigma_{z\theta} + \mathrm{i}\sigma_{zr} \\ -E_r + \mathrm{i}E_\theta \end{bmatrix}^- = \frac{\mathrm{i}}{\sqrt{2\pi r}}\mathbf{MP}\mathrm{Y}(r)\mathbf{K} \quad (r = |\sigma - a|) \tag{67}$$

in the matrix side, where

$$\mathrm{Y}(r) = \begin{bmatrix} r^{-\mathrm{i}\varepsilon} & 0 \\ 0 & r^{\mathrm{i}\varepsilon} \end{bmatrix} \tag{68}$$

$$\mathbf{K} = \mathbf{K}_1 + \mathbf{J}\overline{\mathbf{K}_1} \tag{69a}$$

$$\mathbf{J} = \begin{bmatrix} 0 & 1 \\ 1 & 0 \end{bmatrix} \tag{69b}$$

$$\begin{aligned} \mathbf{K}_1 = {} & \exp\left\{\mathrm{i}\frac{\alpha}{2}\right\}\sqrt{\pi R \sin\alpha} \\ & \times \begin{bmatrix} (1-2\mathrm{i}\varepsilon)\exp\{\mathrm{i}\varepsilon\ln(2R\sin\alpha) + \varepsilon(\alpha - \pi)\} & 0 \\ 0 & (1+2\mathrm{i}\varepsilon)\exp\{-\mathrm{i}\varepsilon\ln(2R\sin\alpha) - \varepsilon(\alpha-\pi)\} \end{bmatrix} \\ & \times (\mathbf{I} + \Lambda)^{-1}\Lambda_1\overline{\mathbf{P}}^{\mathrm{T}}\mathbf{M}(\mathbf{I} + \overline{\mathbf{C}}_2^{-1}\mathbf{C}_2)\mathbf{T} \end{aligned} \tag{69c}$$

Then $\mathbf{K}$ can be defined as a complex electro-elastic field concentration vector to characterize the singular fields near the crack tip. Here we point out that the definition for $\mathbf{K}$ is very similar to that introduced by Willis (1971) for purely anisotropic elastic bimaterials. It follows from Eq. (62) that

$$\Delta\mathbf{U} = \mathbf{U}_1 - \mathbf{U}_2 = -\sqrt{\frac{r}{2\pi}}(\mathrm{e}^{-\pi\varepsilon} + \mathrm{e}^{\pi\varepsilon})\mathrm{P}\begin{bmatrix} \dfrac{1}{1-2\mathrm{i}\varepsilon} & 0 \\ 0 & \dfrac{1}{1+2\mathrm{i}\varepsilon} \end{bmatrix}\mathrm{Y}(r)\mathbf{K} \tag{70}$$

near the upper crack tip.

Following Pak (1990), we can derive the crack extension force G to be of the form

$$G = \frac{1}{8}\overline{\mathbf{K}}^{\mathrm{T}}\begin{bmatrix} \mathrm{e}^{-2\pi\varepsilon}(1+\mathrm{e}^{-2\pi\varepsilon}) & 0 \\ 0 & \mathrm{e}^{2\pi\varepsilon}(1+\mathrm{e}^{2\pi\varepsilon}) \end{bmatrix}\Lambda_1^{-1}\mathbf{K} > 0 \tag{71}$$

During the derivation for G, the local coordinate system (ξ, η) as shown in Fig. 1, which is tangential to the upper crack tip, has been adopted. The right-hand side of Eq. (71) is always positive, reflecting the fact that the linear piezoelectric model predicts a positive driving force for a conducting crack. The positive value of G for a conducting crack is different from that obtained by Pak (1990) for an insulating crack, and is in agreement with that derived by Ru (1999) for a conducting crack parallel to the applied electric field, and is also in accordance with that derived by Govorukha and Loboda (2000) for a conducting crack with a frictionless contact zone.

When condition (36) is met, then stresses, strains, electric fields and electric displacements are singularly distributed just ahead of the upper crack tip along the interface as follows

$$\begin{bmatrix} \gamma_{z\theta} + \mathrm{i}\gamma_{zr} \\ -D_r + \mathrm{i}D_\theta \end{bmatrix}^+ = \frac{\mathrm{i}}{\sqrt{2\pi r}}\mathbf{C}_1^{-1}\widetilde{\mathbf{K}} \quad (r = |\sigma - a|) \tag{72}$$

$$\begin{bmatrix} \sigma_{z\theta} + i\sigma_{zr} \\ -E_r + iE_\theta \end{bmatrix}^+ = \frac{i}{\sqrt{2\pi r}} \widetilde{\mathbf{K}} \quad (r = |\sigma - a|) \tag{73}$$

in the inclusion side, and

$$\begin{bmatrix} \gamma_{z\theta} + i\gamma_{zr} \\ -D_r + iD_\theta \end{bmatrix}^- = \frac{i}{\sqrt{2\pi r}} \mathbf{C}_2^{-1} \widetilde{\mathbf{K}} \quad (r = |\sigma - a|) \tag{74}$$

$$\begin{bmatrix} \sigma_{z\theta} + i\sigma_{zr} \\ -E_r + iE_\theta \end{bmatrix}^- = \frac{i}{\sqrt{2\pi r}} \widetilde{\mathbf{K}} \quad (r = |\sigma - a|) \tag{75}$$

in the matrix side, where

$$\widetilde{\mathbf{K}} = \begin{bmatrix} \widetilde{K}_\sigma \\ \widetilde{K}_E \end{bmatrix} = 2\sqrt{\pi R \sin\alpha}\, \mathbf{M} \mathrm{Re}\{\mathbf{C}_2^{-1}\} \mathrm{Re}\left\{ \exp\left\{ i\frac{\alpha}{2} \right\} \mathbf{C}_2 \mathbf{T} \right\} \tag{76}$$

Taking into mind that $\mathbf{M}$ in Eq. (76) is a real and diagonal matrix. Apparently, the above defined $\widetilde{\mathbf{K}}$ is identical to the conventional definition for field intensity factors (see Deng and Meguid, 1999; Wang and Shen, 2001).

Accordingly,

$$\Delta \mathbf{U} = \mathbf{U}_1 - \mathbf{U}_2 = -2\sqrt{\frac{r}{2\pi}} \mathbf{M}^{-1} \widetilde{\mathbf{K}} \tag{77}$$

near the upper crack tip and the driving force G can be expressed in terms of $\widetilde{\mathbf{K}}$ as follows

$$G = \frac{1}{4} \widetilde{\mathbf{K}}^{\mathrm{T}} \mathbf{M}^{-1} \widetilde{\mathbf{K}} > 0 \tag{78}$$

5. Examples

In order to understand the physical behavior of the obtained solution, we look at some examples. We basically follow the classification for the two-phase piezoelectric composite in Deng and Meguid (1999). In each example, the matrix is subjected to remote uniform mechanical loadings σ_{zx}^∞, σ_{zy}^∞ and remote uniform electrical loadings E_x^∞, E_y^∞.

5.1. An arc crack in a homogeneous piezoelectric material

It follows from Eq. (34) that $\varepsilon = 0$, and as a result all of the physical quantities exhibit the traditional square root singularities. The square root singularities are in agreement with our expectation. Furthermore, it follows from Eq. (76) that

$$\widetilde{\mathbf{K}} = \begin{bmatrix} \tilde{K}_\sigma \\ \tilde{K}_E \end{bmatrix} = \sqrt{\pi R \sin\alpha}\, \mathrm{Re}\left\{ \exp\left\{ i\frac{\alpha}{2} \right\} \begin{bmatrix} \sigma_{zy}^\infty + i\sigma_{zx}^\infty \\ -E_x^\infty + iE_y^\infty \end{bmatrix} \right\} \tag{79}$$

It can be observed from the above expression that $\widetilde{K}_\sigma$ only depends on the crack angle α and remote mechanical loadings; while $\widetilde{K}_E$ only depends on the crack angle α and remote electrical loadings. It is of interest to point out that the above obtained $\tilde{K}_\sigma$ is identical to that derived by Deng and Meguid (1999, Eq. (49.1)) when substituting $\alpha = \pi - \beta$ into Eq. (79). Using Eq. (62), discontinuity in w and φ on the crack L_c can be expressed as

$$\Delta\mathbf{U} = \begin{bmatrix} \Delta w \\ \Delta\varphi \end{bmatrix} = 2\mathrm{Im}\left\{ \sqrt{(\sigma-a)(\sigma-b)} \begin{bmatrix} \dfrac{\sigma_{zy}^{\infty} + \mathrm{i}\sigma_{zx}^{\infty}}{c_{44}^{(2)}} \\ \left(\varepsilon_{11}^{(2)} + \dfrac{e_{15}^{(2)^2}}{c_{44}^{(2)}}\right)(-E_x^{\infty} + \mathrm{i}E_y^{\infty}) \end{bmatrix} \right\}, \quad \sigma \in L_{\mathrm{c}} \tag{80}$$

where the function $\sqrt{(\sigma-a)(\sigma-b)}$ is taken to be the limiting values when approaching the arc crack L_{c} from within the circle $|\sigma| = R$.

We can find that the crack opening displacement Δw only depends on the remote mechanical loadings and is independent of the remote electrical loadings.

5.2. Partially debonded elastic dielectric inclusion in elastic dielectric matrix

In this case, the piezoelectric constants $e_{15}^{(1)} = e_{15}^{(2)} = 0$. It follows from Eq. (34) that $\varepsilon = 0$, and all of the physical quantities will also exhibit the traditional square root singularities. The square root singularities are also in agreement with our expectation. Furthermore, it follows from Eq. (76) that

$$\widetilde{\mathbf{K}} = \begin{bmatrix} \tilde{K}_{\sigma} \\ \tilde{K}_{E} \end{bmatrix} = \sqrt{\pi R \sin\alpha} \begin{bmatrix} \dfrac{2c_{44}^{(1)}}{c_{44}^{(1)} + c_{44}^{(2)}} & 0 \\ 0 & \dfrac{2\varepsilon_{11}^{(2)}}{\varepsilon_{11}^{(1)} + \varepsilon_{11}^{(2)}} \end{bmatrix} \mathrm{Re}\left\{ \exp\left\{\mathrm{i}\frac{\alpha}{2}\right\} \begin{bmatrix} \sigma_{zy}^{\infty} + \mathrm{i}\sigma_{zx}^{\infty} \\ -E_x^{\infty} + \mathrm{i}E_y^{\infty} \end{bmatrix} \right\} \tag{81}$$

It can be found from the above expression that the antiplane elastic fields and the inplane electric fields are decoupled, a conclusion having been similarly drawn by Deng and Meguid (1999). Also, $\tilde{K}_{\sigma}$ is in agreement with that derived by Deng and Meguid (1999, Eq. (51)). In addition, it can be easily verified that $\tilde{K}_{E}$ is in accordance with the result obtained by Deng and Meguid (1999, Eq. (51)). Using Eq. (62), discontinuity in w and φ on the crack L_{c} can be expressed as

$$\Delta\mathbf{U} = \begin{bmatrix} \Delta w \\ \Delta\varphi \end{bmatrix} = 2\mathrm{Im}\left\{ \sqrt{(\sigma-a)(\sigma-b)} \begin{bmatrix} \dfrac{\sigma_{zy}^{\infty} + \mathrm{i}\sigma_{zx}^{\infty}}{c_{44}^{(2)}} \\ \varepsilon_{11}^{(2)}(-E_x^{\infty} + \mathrm{i}E_y^{\infty}) \end{bmatrix} \right\}, \quad \sigma \in L_{\mathrm{c}} \tag{82}$$

From the above equation, we can also observe that antiplane elastic fields and the inplane electric fields are decoupled. Comparing (80) with (82), we deduce that the piezoelectric effect for the matrix will increase the densities of electric charges distributed along the arc crack.

5.3. Partially debonded piezoelectric inclusion in elastic dielectric matrix

In this case, $e_{15}^{(2)} = 0$. It follows from Eq. (34) that

$$\beta = \frac{1}{\sqrt{\left(1 + c_{44}^{(1)}/c_{44}^{(2)}\right)\left[1 + c_{44}^{(1)}(\varepsilon_{11}^{(1)} + \varepsilon_{11}^{(2)})/e_{15}^{(1)^2}\right]}} \tag{83}$$

As a result, the field components will exhibit oscillatory singularities.

5.4. Partially debonded elastic dielectric inclusion in a piezoelectric matrix

In this case, $e_{15}^{(1)} = 0$. It follows from Eq. (34) that

$$\beta = \frac{1}{\sqrt{\left(1 + c_{44}^{(2)}/c_{44}^{(1)}\right)\left[1 + c_{44}^{(2)}\left(\varepsilon_{11}^{(1)} + \varepsilon_{11}^{(2)}\right)\Big/e_{15}^{(2)^2}\right]}} \tag{84}$$

More over, if the inclusion is rigid ($c_{44}^{(1)} \to \infty$), then utilize Eq. (84), we will obtain

$$\beta = \frac{1}{\sqrt{1 + c_{44}^{(2)}\left(\varepsilon_{11}^{(1)} + \varepsilon_{11}^{(2)}\right)\Big/e_{15}^{(2)^2}}} \tag{85}$$

In addition, if the inclusion is also conducting ($\varepsilon_{11}^{(1)} \to \infty$), then utilize Eq. (85), we find that the oscillatory index ε will be zero.

5.5. Partially debonded piezoelectric inclusion in a piezoelectric matrix

In this subsection, we will consider two cases

- $c_{44}^{(1)}e_{15}^{(2)} = c_{44}^{(2)}e_{15}^{(1)}$

  In this special case, the oscillatory index ε will be absent. Utilize Eq. (76), we finally obtain

$$\begin{aligned}\widetilde{K}_\sigma &= \sqrt{\pi R \sin\alpha}\,\frac{2c_{44}^{(1)}}{\left(c_{44}^{(1)} + c_{44}^{(2)}\right)}\mathrm{Re}\left\{\exp\left\{\mathrm{i}\frac{\alpha}{2}\right\}(\sigma_{zy}^\infty + \mathrm{i}\sigma_{zx}^\infty)\right\}\\ \widetilde{K}_E &= \sqrt{\pi R \sin\alpha}\,\frac{2\left(c_{44}^{(2)}\varepsilon_{11}^{(2)} + e_{15}^{(2)^2}\right)}{c_{44}^{(2)}\left(\varepsilon_{11}^{(1)} + \varepsilon_{11}^{(2)}\right) + \left(e_{15}^{(1)} + e_{15}^{(2)}\right)e_{15}^{(2)}}\mathrm{Re}\left\{\exp\left\{\mathrm{i}\frac{\alpha}{2}\right\}(-E_x^\infty + \mathrm{i}E_y^\infty)\right\}\end{aligned} \tag{86}$$

We observe that the stress intensity factor $\widetilde{K}_\sigma$ depends on the remote mechanical loadings and elastic constants of the two-phase system; while $\widetilde{K}_E$ depends on the remote electrical loadings and electro-elastic constants of the two-phase system. In addition, we observe that the above expression for $\widetilde{K}_\sigma$ is identical to Eq. (81). Furthermore, if the matrix is only subjected to mechanical loadings, then it follows from Eq. (78) that the energy release rate has the following simple expression

$$G = \frac{1}{4}\left(\frac{1}{c_{44}^{(1)}} + \frac{1}{c_{44}^{(2)}}\right)\widetilde{K}_\sigma^2 \tag{87}$$

- $c_{44}^{(1)}e_{15}^{(2)} \neq c_{44}^{(2)}e_{15}^{(1)}$

  In this case, we will consider some practical material combinations. We can take PZT-4, PZT-5H, PZT-6B, $BaTiO_3$ and ZnO ceramics as an example of which the engineering material constants are tabulated in Table 1 (Auld, 1973; Chen, 1983; Shindo et al., 1997; Narita and Shindo, 1999).

  The calculated oscillatory index ε are illustrated in Table 2. Note that in the table we only take $\varepsilon > 0$.

Table 1
Material properties of piezoelectric ceramics

No.	Material	c_{44} ($\times 10^{10}$ N/m^2)	e_{15} (C/m^2)	ε_{11} ($\times 10^{-10}$ C/Vm)
1	PZT-4	2.56	12.7	64.6
2	PZT-5H	3.53	17.0	151
3	PZT-6B	2.71	4.6	36
4	$BaTiO_3$	4.3	11.6	112
5	PZT 65/35	3.890	8.387	56.6
6	ZnO	4.247	−0.48	0.757

Table 2
Oscillatory index ε

Combination	ε	Combination	ε	Combination	ε
1 + 2	0.00296287	2 + 3	0.07526100	3 + 5	0.01696536
1 + 3	0.09364796	2 + 4	0.04878082	3 + 6	0.11581951
1 + 4	0.05601788	2 + 5	0.06663201	4 + 5	0.01670386
1 + 5	0.07962070	2 + 6	0.15335673	4 + 6	0.11352178
1 + 6	0.20417562	3 + 4	0.03010062	5 + 6	0.12441863

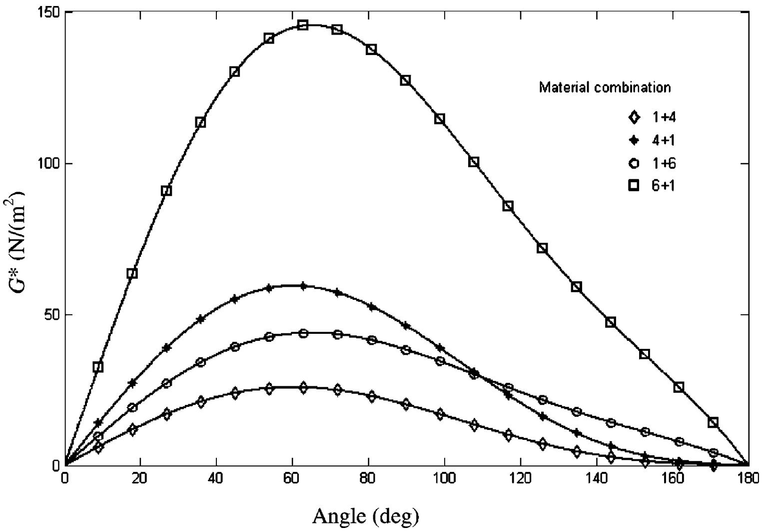

Fig. 2. Variations of the energy release rate $G^* = G/R$ versus crack angle α and some material combinations.

In the Table 2, the number before the sign "+" denotes the inclusion phase, while the number after "+" denotes the matrix phase. We find that the index ε is very small ($\varepsilon < 0.1$) for most of the material combinations. When ZnO is present in the combinations, the index ε is relatively large ($\varepsilon > 0.1$).

We illustrate in Fig. 2 the variations of the energy release rate $G^* = G/R$ versus crack angle α and some material combinations with $\sigma_{zy}^{\infty} = 10^6$ N/m^2, $\sigma_{zx}^{\infty} = 0$, $E_x^{\infty} = -2 \times 10^4$ V/m, $E_y^{\infty} = 0$. We find that different types of material combinations will exert a prominent influence on G, and that the energy release rate will attain a maximum value for a certain angle $0 < \alpha < \pi$ and vanish when $\alpha = 0$ or π. We demonstrate in Fig. 3

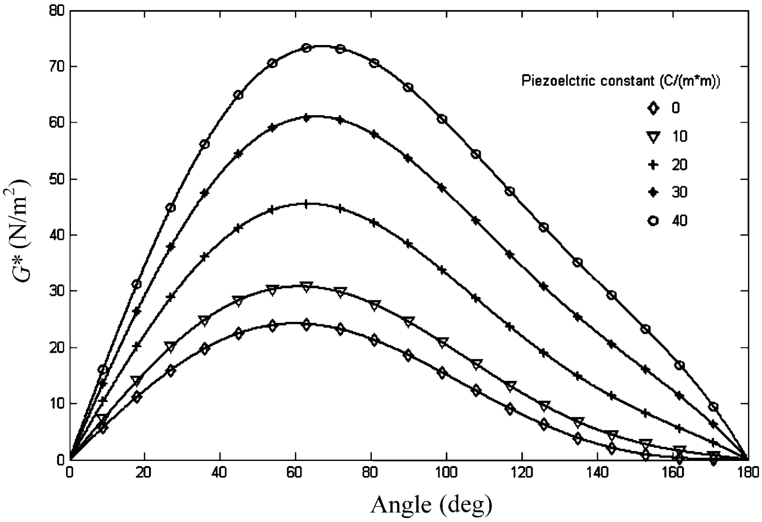

Fig. 3. Variations of the energy release rate $G^* = G/R$ versus crack angle α and the piezoelectric modulus $e_{15}^{(2)}$.

the variations of the energy release rate $G^* = G/R$ versus crack angle α and the piezoelectric modulus $e_{15}^{(2)}$ with $ZnO + BaTiO_3$ combination and $\sigma_{zy}^{\infty} = 10^6$ N/m^2, $\sigma_{zx}^{\infty} = 0$, $E_x^{\infty} = 0$, $E_y^{\infty} = 0$. We find that the energy release rate will increase with the increment of $e_{15}^{(2)}$.

6. Conclusion

The present paper analytically investigates a conducting arc crack between a circular piezoelectric inclusion (inhomogeneity) and an unbounded piezoelectric matrix. The boundary value problem is reduced to a standard Riemann–Hilbert problem of vector form. Closed form solutions for the field potentials are obtained, explicit expressions for distributions of physical quantities are also derived. It is found that all of the physical quantities possess the oscillatory singularities $-(1/2) \pm i\varepsilon$, in which ε is also given explicitly, and that the energy release rate or the driving force is always positive. The formulation presented in Section 2 can also be applied to investigate an insulating curved rigid line between a circular piezoelectric inclusion and an infinite piezoelectric matrix, which is also a stress concentrator and which can be analyzed by an analogous methodology as the interface arc cracks. It should be noted the fact that the rigid line (or anticrack as termed by Dundurs and Markenscoff, 1989) problems in purely elastic media have been extensively investigated by various investigators (see for example, Dundurs and Markenscoff, 1989; Markenscoff et al., 1994; Chen and Hasebe, 1992; Chen, 1996) despite the fact that anticracks do not have applications that are as far ranging as those of cracks, while the rigid line problems in piezoelectric media have not yet been thoroughly investigated.

Acknowledgements

This work was supported by the National Excellent Young Scholar Science Fund of China (Project no. 10125209), the National Natural Science Foundation of China (Project no. 10072041) and the Teaching and Research Award Fund for Outstanding Young Teachers in High Education Institutions of MOE, P.R. China.

Appendix A. Explicit expressions for the constant vector T

Case 1: remote mechanical strains γ_{zx}^{∞}, γ_{zy}^{∞} and remote electric displacement D_x^{∞}, D_y^{∞}

$$\mathbf{T} = \begin{bmatrix} \gamma_{zy}^{\infty} + \mathrm{i}\gamma_{zx}^{\infty} \\ -D_x^{\infty} + \mathrm{i}D_y^{\infty} \end{bmatrix} \tag{A.1}$$

Case 2: remote mechanical stresses σ_{zx}^{∞}, σ_{zy}^{∞} and remote electric fields E_x^{∞}, E_y^{∞}

$$\mathbf{T} = \begin{bmatrix} \dfrac{1}{c_{44}^{(2)}} & -\mathrm{i}\dfrac{e_{15}^{(2)}}{c_{44}^{(2)}} \\ \mathrm{i}\dfrac{e_{15}^{(2)}}{c_{44}^{(2)}} & \varepsilon_{11}^{(2)} + \dfrac{e_{15}^{(2)^2}}{c_{44}^{(2)}} \end{bmatrix} \begin{bmatrix} \sigma_{zy}^{\infty} + \mathrm{i}\sigma_{zx}^{\infty} \\ -E_x^{\infty} + \mathrm{i}E_y^{\infty} \end{bmatrix} \tag{A.2}$$

Case 3: remote mechanical strains γ_{zx}^{∞}, γ_{zy}^{∞} and remote electric fields E_x^{∞}, E_y^{∞}

$$\mathbf{T} = \begin{bmatrix} 1 & 0 \\ \mathrm{i}e_{15}^{(2)} & \varepsilon_{11}^{(2)} \end{bmatrix} \begin{bmatrix} \gamma_{zy}^{\infty} + \mathrm{i}\gamma_{zx}^{\infty} \\ -E_x^{\infty} + \mathrm{i}E_y^{\infty} \end{bmatrix} \tag{A.3}$$

Case 4: remote mechanical stresses σ_{zx}^{∞}, σ_{zy}^{∞} and remote electric displacement D_x^{∞}, D_y^{∞}

$$\mathbf{T} = \begin{bmatrix} \dfrac{\varepsilon_{11}^{(2)}}{c_{44}^{(2)}\varepsilon_{11}^{(2)} + e_{15}^{(2)^2}} & -\mathrm{i}\dfrac{e_{15}^{(2)}}{c_{44}^{(2)}\varepsilon_{11}^{(2)} + e_{15}^{(2)^2}} \\ 0 & 1 \end{bmatrix} \begin{bmatrix} \sigma_{zy}^{\infty} + \mathrm{i}\sigma_{zx}^{\infty} \\ -D_x^{\infty} + \mathrm{i}D_y^{\infty} \end{bmatrix} \tag{A.4}$$

References

Auld, B.A., 1973. Acoustic fields and waves in solids. John Wiley & Sons, New York.

Chen, P.J., 1983. Characterization of the three dimensional properties of poled PZT65/35 in the absence of loses. Acta Mech. 47, 95–106.

Chen, Y.Z., Hasebe, N., 1992. Integral equation approaches for curved rigid line problem in an infinite plate. Int. J. Frac. 58, 1–20.

Chen, Y.Z., 1996. Circular arc rigid line problem with loading on line. ASME J. Appl. Mech. 65, 776–778.

Deng, W., Meguid, S.A., 1999. Closed form solutions for partially debonded circular inclusion in piezoelectric materials. Acta Mech. 137, 167–181.

Dundurs, J., Markenscoff, X., 1989. A green's function formulation of anticracks and their interaction with load-induced singularities. ASME J. Appl. Mech. 56, 550–555.

Govorukha, V.B., Loboda, V.V., 2000. Contact zone models for an interface crack in a piezoelectric material. Acta Mech. 140, 233–246.

Kuo, C.M., Barnett, D.M., 1991. Stress singularities of interfacial cracks in bonded piezoelectric half-spaces. In: Modern Theory of Anisotropic Elasticity and Applications. Wu, J.J., Ting, T.C.T., Barnett, D.M. (Eds.), Philadelphia: SIAM Proceedings series, pp. 33–50.

Markenscoff, X., Ni, L., Dundurs, J., 1994. The interface anticrack and green's functions for interacting anticracks and cracks/anticracks. ASME J. Appl. Mech. 61, 797–802.

Muskhelishvili, N.I., 1953. Some Basic Problems of the Mathematical Theory of Elasticity. Noordhoff, Groningen.

Narita, F., Shindo, Y., 1999. Fatigue crack propagation in a piezoelectric ceramic strip subjected to mode III loading. Acta Mech. 137, 55–63.

Pak, Y.E., 1990. Crack extension force in a piezoelectric material. ASME J. Appl. Mech. 57, 647–653.

Ru, C.Q., 1999. Conducting cracks in a piezoelectric ceramic of limited electrical polarization. J. Mech. Phys. Solids 47, 2125–2146.

Shindo, Y., Tanaka, K., Narita, F., 1997. Singular stress and electric fields of a piezoelectric ceramic strip with a finite crack under longitudinal shear. Acta Mech. 120, 31–45.

Suo, Z., Kuo, C.M., Barnett, D.M., Willis, J.R., 1992. Fracture mechanics for piezoelectric ceramics. J. Mech. Phys. Solids 40, 739–765.

Ting, T.C.T., 1986. Explicit solution and invariance of the singularities at an interface crack in anisotropic composites. Int. J. Solids Struct. 22, 965–983.

Wang, X., Shen, Y.P., 2001. Arc interface crack in a three-phase piezoelectric composite constitutive model. Acta Mechanica Solida Sinica 14, 104–117.

Willis, J.R., 1971. Fracture mechanics of interfacial cracks. J. Mech. Phys. Solids 19, 353–368.

Zhong, Z., Meguid, S.A., 1997. Interfacial debonding of a circular inhomogeneity in piezoelectric materials. Int. J. Solids Struct. 34, 1965–1984.